Published in final edited form as:
*Ultrasound Med Biol*. 2014 January ; 40(1): 130–137. doi:10.1016/j.ultrasmedbio.2013.09.015.

# Microbubble Type and Distribution Dependence of Focused Ultrasound Induced Blood Brain Barrier Opening

**Shutao Wang**[1], **Gesthimani Samiotaki**[1], **Oluyemi Olumolade**[1], **Jameel A. Feshitan**[1], and **Elisa E. Konofagou**[1,2]

[1]Ultrasound and Elasticity Imaging Laboratory, Department of Biomedical Engineering, Columbia University, New York, NY, USA

[2]Department of Radiology, Columbia University, New York, NY, USA

## Abstract

Focused Ultrasound (FUS) in the presence of microbubbles has been used to non-invasively induce reversible blood brain barrier (BBB) opening in both rodents and non-human primates. This study aims at identifying the dependence of the BBB opening properties on the polydisperse microbubble (since all clinically approved microbubbles are polydisperse) type and distribution by using clinically approved UCA (Definity®) and in-house made polydisperse microbubbles (IHP) in mice. A total of 18 C57BL/6 mice (n = 3) were used in this study, and each mouse received either Definity® or IHP microbubbles via tail vein injection. The concentration and size distribution of both the activated Definity® and IHP microbubbles were measured and diluted to $6\times10^8$/ml prior to injection. Immediately after the microbubble administration, FUS sonications were carried out with the following parameters: frequency of 1.5 MHz, pulse repetition frequency of 10 Hz, 1000 cycles, in situ peak rarefactional acoustic pressures of 0.3 MPa, 0.45 MPa, and 0.6 MPa for a sonication duration of 60 s. Contrast-enhanced magnetic resonance imaging (MRI) was used to confirm the BBB opening and allowed for image-based analysis. The permeability of the treated region and volumes of BBB opening using the two types of microbubbles did not show significant difference ($P > 0.05$) for PRPs of 0.45 MPa and 0.6 MPa, while IHP microbubbles showed significantly higher permeability and volume of opening ($P < 0.05$) at the relatively lower pressure of 0.3 MPa. The results from this study indicate that the microbubble type and distribution could have significant effects on the FUS-induced BBB opening at lower, but less important at higher, pressure levels, possibly due to the stable cavitation that governs the former. This difference may have become less significant at higher FUS pressure levels where inertial cavitation typically occurs.

### Keywords

Blood-brain Barrier opening; Focused Ultrasound; Microbubble Type and Distribution



Address correspondence to: Elisa E. Konofagou, Ph.D., Department of Biomedical Engineering, Columbia University, 351 Engineering Terrace, mail code 8904, 1210 Amsterdam Avenue, New York, NY 10027. ek2191@columbia.edu.

## INTRODUCTION

One of the main obstacles for the treatment of neurodegenerative diseases (e.g. Parkinson's disease and Alzheimer's disease) is the blood brain barrier (BBB). While the primary function of the BBB is to prevent toxins from entering the brain parenchyma, it also impedes the delivery of therapeutic agents with the size of 400 Da and above (Pardridge, 2005). Different strategies have been proposed to temporarily disrupt the BBB, including hyperosmolar solutions (such as mannitol) and focused ultrasound (FUS) in combination with microbubbles. In contrast to the hyperosmolar methods, FUS in the presence of microbubbles was demonstrated to be the only non-invasive approach capable of temporarily opening the BBB in the targeted region (Hynynen et al., 2001; Choi et al., 2007). Using carefully selected acoustic parameters, FUS-induced BBB opening was shown to be safe in both rodents (Baseri et al., 2010) and non-human primates (Marquet et al., 2011; Tung et al., 2011a; McDannold et al., 2012).

Although the exact mechanism is still not completely understood, the interaction between capillary walls and acoustically driven microbubbles was shown to be one of the key factors that lead to the disruption of the BBB (Tung et al., 2011b). Until now, most studies have utilized the commercially available and United States Food and Drug Administration (FDA) approved ultrasound contrast agents (UCA). These include protein-coated UCA Optison™ (Choi et al., 2007; McDannold et al., 2008) and lipid coated UCA Definity® (Tung et al., 2011b; McDannold et al., 2012). Compared to the protein-coated UCA, the lipid-based microbubbles are formed by self-assembled monolayer phospholipids and are more responsive to ultrasound compared to protein-coated microbubbles (Sirsi and Borden, 2009). Definity® microbubbles are highly polydisperse agents with bubble diameters ranging from submicron to above 10 μm. As a result, the resonant frequencies of these bubbles cover a wide range on the spectrum (above 10 MHz) (Goertz et al., 2007; Cheung et al., 2008). Using Definity® microbubbles, Baseri et al. (2010) evaluated the BBB opening threshold and safest acoustic pressure ranges in mice at 1.525 MHz. The acoustic pressure window of 0.3 – 0.46 MPa was determined to be safe with the parameters used in that study (pulse length of 20 ms, pulse repetition frequency of 10 Hz).

In this study, we aimed at comparing the Definity® and in-house polydisperse (IHP) microbubbles, both of which are formed by high shear gas dispersion in an aqueous lipid-shell mixture. Although these two microbubbles have similar compositions, their behavior for the application of FUS-induced BBB opening has not been studied. The two main motivations for this study were to: 1) evaluate whether Definity® and IHP microbubbles have similar effects on the BBB opening characteristic, and 2) determine whether IHP can serve as a surrogate for commercially available microbubble Definity®. The efficiency of BBB opening using these microbubbles was evaluated by analyzing the increase in brain tissue permeability and the total volume of BBB opening. The microbubble type dependence was evaluated at different *in situ* acoustic pressures, ranging from 0.3 to 0.6 MPa. Tung et al. (UMB 2010) showed (using Definity® microbubbles) that inertial cavitation occurred at 0.45 MPa and 0.6 MPa, but not at 0.3 MPa in mice. Therefore, the FUS parameters selected in this study covered both stable and inertial cavitation regimes for Definity® microbubbles. Finally, the BBB reversibility was monitored and histological observations of the brains were performed for safety evaluation.

## METHODS

### Microbubbles

As indicated previously, two types of microbubbles were used in this study: Definity® (Lantheus Medical Imaging, N. Billerica, MA) and IHP microbubbles. Definity® vials,

which are primarily composed of an aqueous solution of lipids and octofluoropropane ($C_3F_8$) gas, were stored at 4 °C prior to use. Immediately before sonications, Definity® vials were activated (at an initial temperature of 4 °C) via mechanical agitation using VialMix™ (Lantheus Medical Imaging, N. Billerica, MA) shaker for a pre-set time of 45 s. The IHP microbubbles were manufactured according to a previously published protocol (Feshitan et al., 2009). Briefly, the 1,2-distearoyl-sn-glycero-3-phosphocholine (DSPC) and polyethylene Glycol 2000 (PEG2000) were mixed at a 9:1 ratio. Ten milligram of the mixture was dissolved in a 10 ml solution consisted of filtered PBS/glycerol (10% volume)/ propylene glycol (10% volume) using a sonicator (model 1510, Branson Ultrasonics, Danbury, CT, USA). Each IHP microbubble vial (total volume of 5 ml) contained 2-mL lipid solution and the vial was sealed and stored at 4°C. Prior to activation, the air in the IHP vial was vacuumed out via a 26G needle and the head space of the vial was filled with decafluorobutane ($C_4F_{10}$) gas. This vacuuming-filling procedure was repeated 5 times for each vial to ensure high $C_4F_{10}$ concentration. The vial was then activated via a VialMix™ shaker for 45 s.

Immediately after activation, the concentration and size distribution of each microbubble vial were measured with a Coulter Counter Multisizer (Beckman Coulter Inc., Fullerton, CA), which measures microbubbles in a range of 0.6 – 18 μm. The microbubbles were then diluted in sterile saline (Vedco Inc. Saint Joseph, MO), yielding a concentration of approximately $6\times10^8$ number of bubbles per mL.

## Preparation of Animals

A total of 18 mice (Strain: C57BL/6, Harlan, Indianapolis, IN) were used in this study. Each mouse was anesthetized with a mixture of oxygen and 1–3% isoflurane (SurgiVet, Smiths Medical PM, Inc., WI) and placed prone with its head immobilized by a stereotaxic apparatus (David Kopf Instruments, Tujunga, CA). The hair on the mouse head was removed by an electrical trimmer and depilatory cream to minimize impedance mismatch. All procedures involving animals were approved by the Columbia University Institutional Animal Care and Use Committee.

## Sonication Protocol and MRI Imaging

A single element FUS transducer (focal length: 60 mm and radius: 30 mm, Imasonic, France) with a center frequency of 1.5 MHz was used for all sonications. A pulse-echo transducer (radius: 11.2 mm, focal length: 60 mm, and center frequency: 10 MHz, Olympus NDT, Waltham, MA) was confocally mounted at the center opening (diameter 11.2 mm) of the FUS transducer (Vlachos et al., 2010). A piece of polyurethane membrane (Trojan; Church & Dwight Co., Inc., Princeton, NJ) was used to seal the transducer cone, which was filled with de-ionized and degassed water. The transducer system was attached to a computer controlled three-dimensional positioner (Velmex Inc., Lachine, QC, Canada). The FUS transducer was connected to a matching circuit and driven by a computer controlled function generator (Agilent, Palo Alto, CA) and a 50 dB power amplifier (ENI Inc., Rochester, NY). The pulse-echo transducer was driven by a pulser-receiver (Olympus, Waltham, MA), which was connected to a digitizer (Gage Applied technologies, Inc., Lachine, QC, Canada) for data acquisition. The −6dB focal zone of the FUS transducer was measured by a needle hydrophone (Precision Acoustics Ltd., Dorchester, UK) in degassed water to be 7.5 mm × 1 mm.

In this study, the FUS beam was targeted at the right hippocampus, while the left side served as control. The targeting was achieved using a grid and the procedure has been described in great detail elsewhere (Choi et al., 2007). The FUS focus was placed 3 mm below the skull, and 18% attenuation was accounted for acoustic pressure loss through the skull (Choi et al.,

2008). With each type of microbubble (Definity® or IHP microbubbles), a bolus of 1 μl/g diluted microbubbles ($6\times10^8$ number per mL) was injected intravenously through the tail vein immediately before sonication. Each vial of microbubbles was used for three mice after activation. *In situ* peak rarefractional acoustic pressures (PRP) used in this study were estimated to be 0.30, 0.45, and 0.60 MPa, and three mice were sonicated at each PRP level. The pulsed FUS was applied with a pulse repetition frequency of 10 Hz, 1000 cycles, and a total duration of 60 seconds.

Upon completion of the FUS sonication (with an intervening delay of 15 min due to animal transfer), the BBB opening was confirmed with a 9.4T MRI system (Broker Medical, Boston, MA). The mice were placed in a birdcage coil (diameter 3 cm), while being anesthetized with 1 – 2% isoflurane and vital sign monitored throughout the imaging sessions. On Day 0, dynamic contrast enhanced (DCE) MR images were collected before and after an intraperitoneal injection of 0.3 mL gadodiamide (GD-DTPA) (Omniscan®, GE Healthcare, Princeton, NJ). Approximately 55 min after the injection, an additional post-contrast enhancement, T1-weighted 2D FLASH acquisition was performed (Vlachos et al., 2010). The BBB opening volume was monitored with the post-contrast T1-weighted imaging until the opening volume reduced to less than 1 $mm^3$, i.e. up to 3 days following initial sonication.

Seven days after FUS, all mice were sacrificed and transcardially perfused with 30 mL PBS and 60 mL 4% paraformaldehyde. The brains were then soaked in paraformaldehyde for 24 hours followed by skull removal and fixation in paraformaldehyde. Hematoxylin and eosin (H&E) staining was performed on the paraffin-embedded brain tissues with a slice thickness of 6 μm for histological examinations.

## Image Analysis

The permeability of the BBB-opened region was analyzed based on the DCE MR images using the general kinetic model (GKM). The detailed description of the methodology can be found elsewhere (Vlachos et al., 2010). Briefly, a two-compartment model was constructed, which included the blood plasma and extracellular space (EES) as follows:

$$\frac{dC_t}{dt}=K_{trans}C_p-K_{ep}C_t \quad (1)$$

where $K_{trans}$ and $K_{ep}$ are the transfer rate constants from the blood plasma to the EES and from the EES to the blood plasma, respectively. $C_p$ and $C_t$ represent the concentrations of Gd-DTPA in the blood plasma and the EES. The signal intensity in the DCE T1-weighted images was translated to GD-DTPA concentration with the Solomon-Bloembergen equation (Parker and Buckley, 2005). The model was solved using the Levenberg-Marquardt fitting algorithm (MATLAB R2011a, MathWorks, Inc., Natick, MA).

The volume of BBB opening was quantitatively determined with volumetric measurements of post-contrast T1-weighted MR images (Samiotaki et al., 2012). The T1-weighted images had a resolution of 86 × 86 $\mu m^2$ and slice thickness of 500 μm (23 slices per scan, no inter-slice gap). The BBB-opened region was segmented (intensity higher than 2.5 standard deviations of the background) with a manually positioned elliptic cylinder (major diameter 4.3 mm, minor diameter 3.4 mm, and height 4.5 mm) over the right hippocampus following the shape of the focal spot in that plane. An additional elliptic cylinder of the same size was placed on the unsonicated (left) side of the brain. Voxels above the segmentation threshold on the unsonicated side were subtracted from the sonicated side to exclude the vessels and ventricles.

### Statistics

Statistical analyses were carried out to compare the dependence of BBB opening on microbubble types at all three PRP levels. Student's t-tests were performed to analyze the permeability and the volume of BBB opening between the two types of microbubbles used in this study. The BBB closing timeline was compared with one-way ANOVA followed by a *post hoc* Tukey's Honestly Significant Difference (HSD) test. A p-value less than 0.05 was considered to be statistical significant.

## RESULTS

The size distributions of Definity® and the IHP microbubbles (n = 3) are shown in Fig. 1. The majority (more than 99%) of both types of microbubbles had diameters of 8 μm or less as indicated in Fig. 1a. Nonetheless, the volume percentage (Fig. 1b) of the Definity® microbubbles slightly peaked around 3 μm, while that of the IHP microbubbles gradually reached a plateau around 5 μm.

The BBB opening was revealed as the contrast-enhanced region (hippocampus on the right side) in the post-contrast MR images (Fig. 2). The permeability ($K_{trans}$) values, ranging from 0 – 0.04 $min^{-1}$, were overlaid onto the MR images. Sample permeability maps of FUS sonicated brains using IHP and Definity® microbubbles are shown in Fig. 2. The permeability averaged over the BBB-opened region was compared between the two-microbubble types across the PRP levels used in this study (Fig. 3). No statistically significant difference ($p > 0.05$) was found between groups injected with Definity® and IHP microbubbles when sonicated with 0.45 MPa and 0.6 MPa. Nevertheless, the permeability of BBB-opened regions using IHP microbubbles was significantly higher ($p < 0.01$) than that of the Definity® injected group at 0.3 MPa.

A similar trend was observed from the BBB opening volume comparisons, as shown in Fig. 4. Although the mean opening volumes from the groups injected with IHP microbubbles are larger than the corresponding groups injected with Definity®, the statistical significant difference ($p = 0.027$) only occurred at 0.3 MPa.

The BBB closing (i.e. BBB opening volume on each subsequent day) timelines of all the tested groups are plotted in Fig. 5. With the sonication parameters used in this study, the BBB of all mice closed within 3 days after treatment. Comparisons were made between groups using the two types of microbubbles at each PRP level. At PRPs of 0.45 MPa and 0.6 MPa, no significant difference (Tukey's HSD test, $p > 0.05$) was observed between groups using Definity® (black) and IHP (red) microbubbles groups on day 0 as well as the following days. The BBB opening volumes were found to be significantly different (Tukey's HSD test, $p < 0.05$) for the groups sonicated at 0.3 MPa on Day 0, but not thereafter.

The safety of BBB opening was evaluated by detecting red blood cell (RBC) extravasation and dark neurons in histological images. H&E stained brain slides (Fig. 6) revealed that there were no damage in the Definity® injected groups at all ultrasound exposures used in this study. Among all the groups injected with IHP microbubbles, several dark neurons were detected in only one mouse (sonicated at 0.45 MPa). No damage was observed in any other mice injected with IHP microbubbles, including the ones sonicated at 0.6 MPa.

## DISCUSSION

Focused ultrasound, in the presence of microbubbles, has been shown to be capable of disrupting the targeted BBB in mice and non-human primates (Choi et al., 2007; Tung et al., 2011a; McDannold et al., 2012). Most recently, transcranial FUS was applied in clinical

trials for the treatments of essential tremor in the US (Elias, 2011) and Canada (Lipsman et al., 2013). These results have promised FUS an attractive role in the future treatments of neurodegenerative diseases such as Parkinson's disease and Alzheimer's disease. The interaction between FUS-driven microbubbles and surrounding blood vessels is a complicated phenomenon, which still requires extensive investigations from all perspectives (Wiedemair et al., 2012). In the present study, we primarily focused on the microbubble type dependence of the BBB opening. Injected with either Definity® or IHP microbubbles, to represent the polydispersity of microbubbles currently approved in the clinic, mice were sonicated with distinct PRPs of 0.3 MPa, 0.45 MPa, and 0.6 MPa. Despite the differences of lipid-shell material and gas core content, it was concluded from MRI-based analysis that there were no significant differences in permeability and volume of opening using these two types of microbubbles when sonicated at relatively high PRPs (0.45 MPa and 0.6 MPa). Interestingly, both of these parameters revealed significant difference once the FUS PRP was lowered to 0.3 MPa (Figs 3&4). Histological examinations also indicated that neither of these two types of microbubbles induced damage when mice were sonicated at 0.3 and 0.6 MPa. A minor injury (several dark neurons) was detected in 1 out of 9 mice from the IHP group (sonicated at 0.45 MPa).

The discrepancy at 0.3 MPa can be explained, in part, by analyzing the microbubble size distributions (Fig. 1). Vlachos et al. (2011) investigated the effect of microbubble diameters on the BBB opening, where monodispersed microbubbles (diameters: 1 – 2 μm, 4 – 5 μm, and 6 –8 μm) were used during FUS sonications. They found that microbubbles with diameters of 1 – 2 μm resulted in significantly lower permeability enhancement compared to the relatively larger microbubbles (4 – 5 μm and 6 – 8 μm). In addition, Samiotaki et al. (2012) reported the BBB opening recovery time with 1 – 2 μm microbubbles was shorter than that of the relatively larger ones. As illustrated in Fig. 1b, although both types of microbubbles exhibited polydispersity, the volumetric size distribution varied across different diameter ranges. Definity ® contained slightly higher volume of 2 – 4 μm microbubbles, whereas the IHP microbubbles consisted of a relatively higher volume of 4 – 8 μm microubbles (Fig. 1). While no significant difference was concluded using these two types of microbubbles at higher pressures (0.45 MPa and 0.6 MPa), this size distribution difference, albeit small, might have become important at lower pressure levels. Luan et al. (2012) showed that at a resonant frequency of 1.5 MHz, the corresponding microbubble diameter is approximately 5–6 μm. Therefore, even though the number fraction of 2 – 4 μm microbubbles in Definity® was higher than that in IHP, the 5 – 8 μm microbubbles (higher number fraction in IHP) might have a better chance to interact with capillary walls at 0.3 MPa. Whereas at relatively higher driving pressures, microbubbles with a much wider diameter range contributed to the BBB opening, resulting in the insignificant permeability and opening volume at 0.45 MPa and 0.6 MPa.

Passive cavitation detection (PCD) has been previously used to study the microbubble response under sonication both in vitro and in vivo (Tung et al., 2010; Tung et al., 2011a; Arvanitis et al., 2012). Particularly, Tung et al. (2010) reported the cavitation effects in mice using Definity® microbubbles and the PRP ranged from 0.3 MPa to 0.9 MPa. It was observed that only stable cavitation occurred at 0.3 MPa for the BBB-opened mice. Once the PRP reached 0.45 MPa or higher, a broadband response (inertial cavitation) was detected (Tung et al., 2010). Therefore, the similar permeability and volume of BBB opening findings at 0.45 MPa and 0.6 MPa were presumed to be caused by the dominating inertial cavitation effects for both Definity® and IHP microbubbles. On the contrary, the BBB opening at 0.3 MPa was mainly attributed to the stable cavitation (i.e. microbubble oscillations) effects. At this pressure level, the relatively large (4 – 8 μm) microbubbles had higher chances to interact with the capillaries (diameter around 7 μm) while oscillating. Therefore, the slightly higher 4 – 8 μm components presented in IHP microbubbles might

have contributed to the significantly different permeability and volume of opening at 0.3 MPa. Therefore, the IHP microbubbles may be considered more efficient for FUS induced BBB opening compared to Definity®, especially when only stable cavitation or maximal safety is required.

There are several limitations in the current study. The number of animals was three per group, which might have induced some uncertainties to the results. Another limitation is that no cavitation detection was performed in this study and the stable and inertial cavitation thresholds for IHP microbubbles remain unknown. Therefore, the interpretation of our results relied on the previously published work (Tung et al., 2010; Tung et al., 2011b), which was done with Definity® Microbubbles and monodisperse microbubbles, respectively. In addition to the effect of size distribution difference between the two types of microbubbles used in this study, the different lipid-shell materials or gas contents may also contribute to the BBB opening differences (Tung et al., 2012). Furthermore, the pre-activation temperature was recently reported to affect the Definity® distribution (Helfield et al., 2012). In this study, Definity® was activated at approximately 4°C, while the IHP microbubble underwent $C_4F_{10}$ gas change before activation (which might bring the vial temperature close to room temperature). The effect of pre-activation temperatures of microbubble vials on the BBB opening is being investigated in our ongoing studies.

## CONCLUSION

This study evaluated the FUS induced BBB opening in the presence of Definity® or in-house polydisperse microbubbles. The microbubble type dependence was investigated by comparing the permeability of sonicated brain and total volume of opening between the two-microbubble types. No significant difference was observed at PRPs at or above 0.45 MPa while at 0.3 MPa, the BBB opening volume and permeability were significantly higher with the IHP microbubbles. The study suggests IHP microbubbles may be more efficient in for FUS induced BBB opening compared to Definity® microbubbles.

## Acknowledgments

This study was supported in part by NIH R01EB009041, NIH R01AG038961, the Wallace H. Coulter and the Kinetics Foundations. The authors appreciate Cherry Chen, Ph.D. and Yao-Sheng Tung, Ph.D. from our laboratory for insightful discussions.

## References

Arvanitis CD, Livingstone MS, Vykhodtseva N, McDannold N. Controlled ultrasound-induced blood-brain barrier disruption using passive acoustic emissions monitoring. PloS one. 2012; 7:e45783. [PubMed: 23029240]

Baseri B, Choi JJ, Tung YS, Konofagou EE. Multi-modality safety assessment of blood-brain barrier opening using focused ultrasound and definity microbubbles: a short-term study. Ultrasound in medicine & biology. 2010; 36:1445–59. [PubMed: 20800172]

Cheung K, Couture O, Bevan PD, Cherin E, Williams R, Burns PN, Foster FS. In vitro characterization of the subharmonic ultrasound signal from Definity microbubbles at high frequencies. Physics in medicine and biology. 2008; 53:1209–23. [PubMed: 18296758]

Choi JJ, Pernot M, Small SA, Konofagou EE. Noninvasive, transcranial and localized opening of the blood-brain barrier using focused ultrasound in mice. Ultrasound in medicine & biology. 2007; 33:95–104. [PubMed: 17189051]

Choi JJ, Wang S, Brown TR, Small SA, Duff KE, Konofagou EE. Noninvasive and transient blood-brain barrier opening in the hippocampus of Alzheimer's double transgenic mice using focused ultrasound. Ultrasonic imaging. 2008; 30:189–200. [PubMed: 19149463]

Elias WJH, D.; Khaled, M. MR Guided Focused Ultrasound Lesioning for the Treatment of Essential Tremor. A New Paradigm for Noninvasive Lesioning and Neuromodulation. Congress of Neurological Surgeons 2011 Annual Meeting; Washington, DC. 2011.

Feshitan JA, Chen CC, Kwan JJ, Borden MA. Microbubble size isolation by differential centrifugation. Journal of colloid and interface science. 2009; 329:316–24. [PubMed: 18950786]

Goertz DE, de Jong N, van der Steen AF. Attenuation and size distribution measurements of Definity and manipulated Definity populations. Ultrasound in medicine & biology. 2007; 33:1376–88. [PubMed: 17521801]

Helfield BL, Huo X, Williams R, Goertz DE. The effect of preactivation vial temperature on the acoustic properties of Definity. Ultrasound in medicine & biology. 2012; 38:1298–305. [PubMed: 22502892]

Hynynen K, McDannold N, Vykhodtseva N, Jolesz FA. Noninvasive MR imaging-guided focal opening of the blood-brain barrier in rabbits. Radiology. 2001; 220:640–6. [PubMed: 11526261]

Lipsman N, Schwartz ML, Huang Y, Lee L, Sankar T, Chapman M, Hynynen K, Lozano AM. MR-guided focused ultrasound thalamotomy for essential tremor: a proof-of-concept study. Lancet neurology. 2013; 12:462–8. [PubMed: 23523144]

Luan Y, Faez T, Gelderblom E, Skachkov I, Geers B, Lentacker I, van der Steen T, Versluis M, de Jong N. Acoustical properties of individual liposome-loaded microbubbles. Ultrasound in medicine & biology. 2012; 38:2174–85. [PubMed: 23196203]

Marquet F, Tung YS, Teichert T, Ferrera VP, Konofagou EE. Noninvasive, transient and selective blood-brain barrier opening in non-human primates in vivo. PloS one. 2011; 6:e22598. [PubMed: 21799913]

McDannold N, Arvanitis CD, Vykhodtseva N, Livingstone MS. Temporary disruption of the blood-brain barrier by use of ultrasound and microbubbles: safety and efficacy evaluation in rhesus macaques. Cancer research. 2012; 72:3652–63. [PubMed: 22552291]

McDannold N, Vykhodtseva N, Hynynen K. Effects of acoustic parameters and ultrasound contrast agent dose on focused-ultrasound induced blood-brain barrier disruption. Ultrasound in medicine & biology. 2008; 34:930–7. [PubMed: 18294757]

Pardridge WM. The blood-brain barrier: bottleneck in brain drug development. NeuroRx : the journal of the American Society for Experimental Neuro Therapeutics. 2005; 2:3–14.

Parker, G.; Buckley, D. Tracer Kinetic Modelling for $T_1$-Weighted DCE-MRI Dynamic Contrast-Enhanced Magnetic Resonance Imaging in Oncology. Jackson, A.; Buckley, D.; Parker, G., editors. Springer; Berlin Heidelberg: 2005. p. 81-92.

Samiotaki G, Vlachos F, Tung YS, Konofagou EE. A quantitative pressure and microbubble-size dependence study of focused ultrasound-induced blood-brain barrier opening reversibility in vivo using MRI. Magnetic resonance in medicine : official journal of the Society of Magnetic Resonance in Medicine / Society of Magnetic Resonance in Medicine. 2012; 67:769–77. [PubMed: 21858862]

Sirsi S, Borden M. Microbubble Compositions, Properties and Biomedical Applications. Bubble science engineering and technology. 2009; 1:3–17. [PubMed: 20574549]

Tung YS, Marquet F, Teichert T, Ferrera V, Konofagou EE. Feasibility of noninvasive cavitation-guided blood-brain barrier opening using focused ultrasound and microbubbles in nonhuman primates. Applied physics letters. 2011a; 98:163704. [PubMed: 21580802]

Tung YS, Vlachos F, Choi JJ, Deffieux T, Selert K, Konofagou EE. In vivo transcranial cavitation threshold detection during ultrasound-induced blood-brain barrier opening in mice. Physics in medicine and biology. 2010; 55:6141–55. [PubMed: 20876972]

Tung YS, Vlachos F, Feshitan JA, Borden MA, Konofagou EE. The mechanism of interaction between focused ultrasound and microbubbles in blood-brain barrier opening in mice. The Journal of the Acoustical Society of America. 2011b; 130:3059–67. [PubMed: 22087933]

Tung, YS.; Olumolade, OO.; Wang, S.; Wu, SY.; Konofagou, EE. Physical mechanism of non-inertial cavitation induced blood-brain barrier opening using focused ultrasound and microbubbles. 12th International Symposium on Therapeutic Ultrasound; Heidelberg, Germany. 2012.

Vlachos F, Tung YS, Konofagou E. Permeability dependence study of the focused ultrasound-induced blood-brain barrier opening at distinct pressures and microbubble diameters using DCE-MRI.

Magnetic resonance in medicine : official journal of the Society of Magnetic Resonance in Medicine / Society of Magnetic Resonance in Medicine. 2011; 66:821–30. [PubMed: 21465543]

Vlachos F, Tung YS, Konofagou EE. Permeability assessment of the focused ultrasound-induced blood-brain barrier opening using dynamic contrast-enhanced MRI. Physics in medicine and biology. 2010; 55:5451–66. [PubMed: 20736501]

Wiedemair W, Tukovic Z, Jasak H, Poulikakos D, Kurtcuoglu V. On ultrasound-induced microbubble oscillation in a capillary blood vessel and its implications for the blood-brain barrier. Physics in medicine and biology. 2012; 57:1019–45. [PubMed: 22298199]

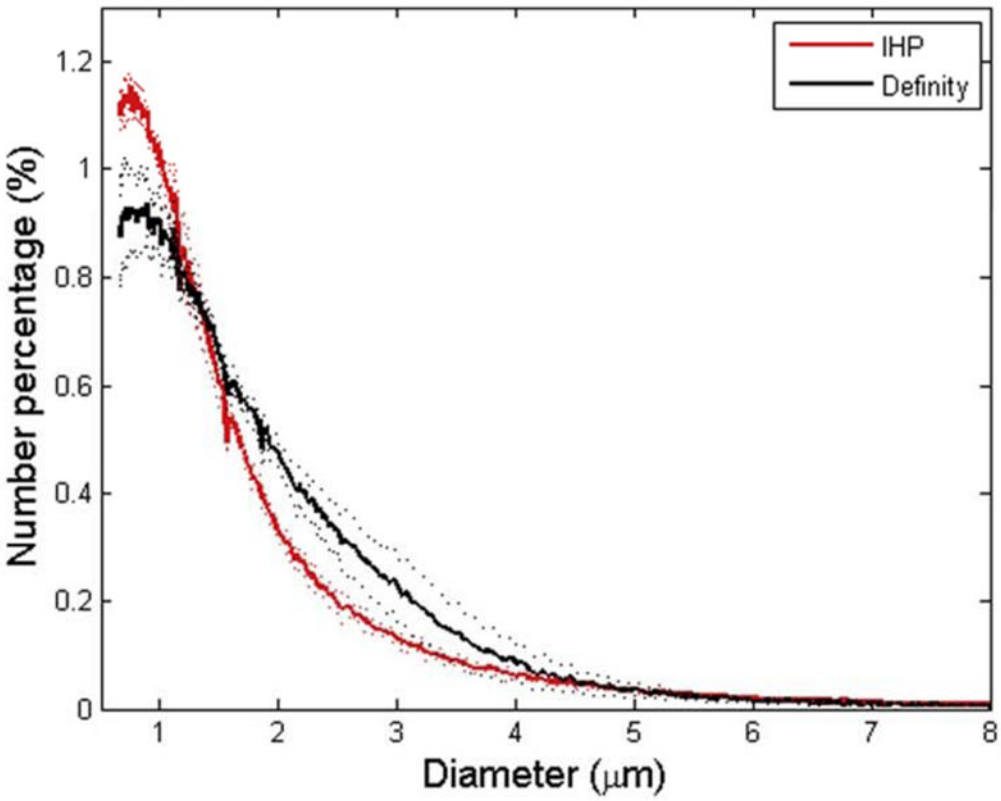

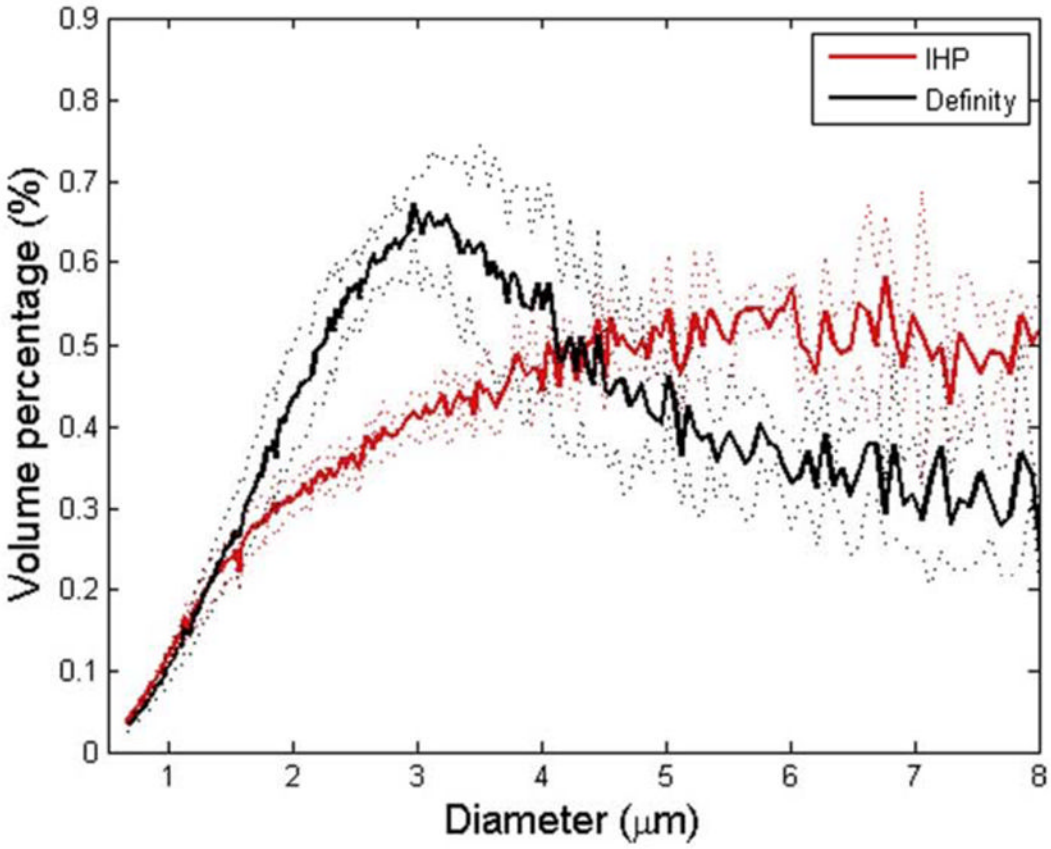


**Figure 1.**
Size distributions for Definity® and IHP microbubbles. The mean distribution data (averaged over 3 vials) and ± standard deviation (dotted lines) are plotted. (a) Number percentage vs. microbubble diameter; (b) volume percentage vs. microbubble diameter.

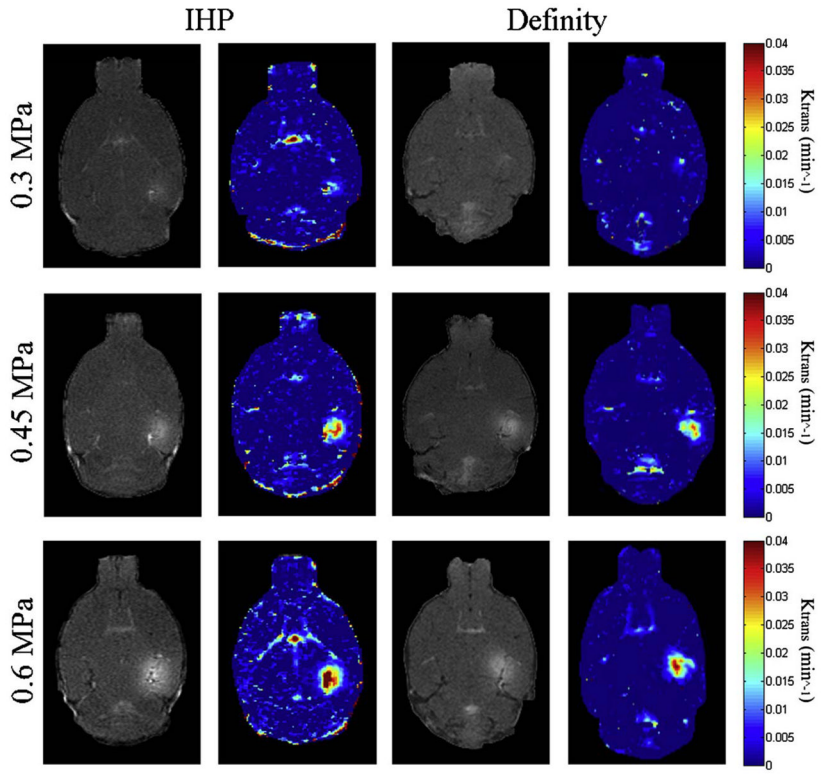


**Figure 2.**
Post-contrast enhanced T1-weighted MR images and corresponding permeability maps of mice injected with in-house polydisperse (IHP) and Definity® microbubbles.

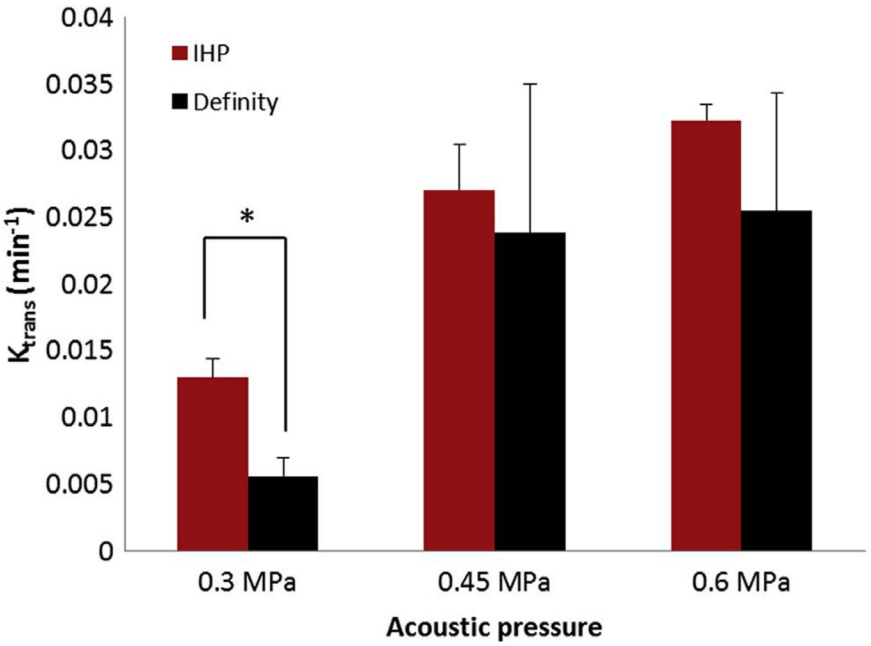


**Figure 3.**
Permeability measurements for mice (n = 3) injected with Definity® (black) and in-house polydisperse (IHP) microbubbles (red) with various sonication peak rarefactional pressures (PRPs). Significant difference (T-test, $p < 0.01$) was found only between the two groups sonicated at the PRP of 0.3 MPa (indicated by asterisk).

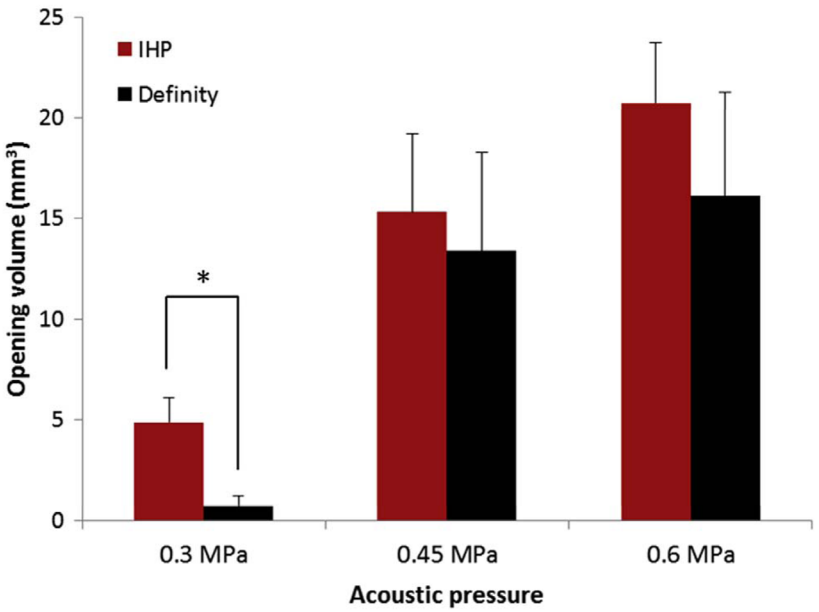


**Figure 4.**

The BBB opening volumes for mice (n = 3) injected with Definity® (black) and in-house polydisperse (IHP) microbubbles (red) with various sonication peak rarefactional pressures (PRPs). Significant difference (T-test, p = 0.027) was found only between the two groups sonicated at the PRP of 0.3 MPa (indicated by asterisk).

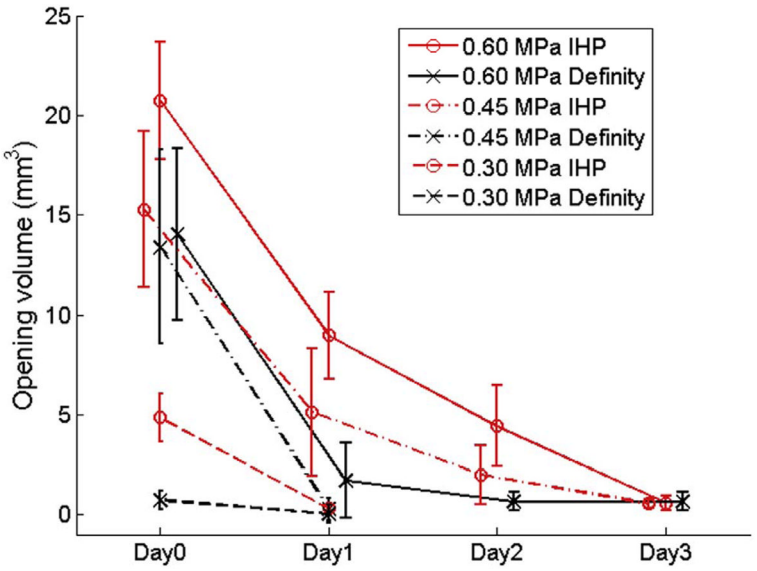


**Figure 5.**
The BBB closing timelines for Definity® (black) and in-house polydisperse (IHP) microbubbles (red) injected mice, and sonicated at peak rarefactional pressures (PRPs) of 0.3 MPa (dashed lines), 0.45 MPa (dash-dot lines), and 0.6 MPa (solid lines).

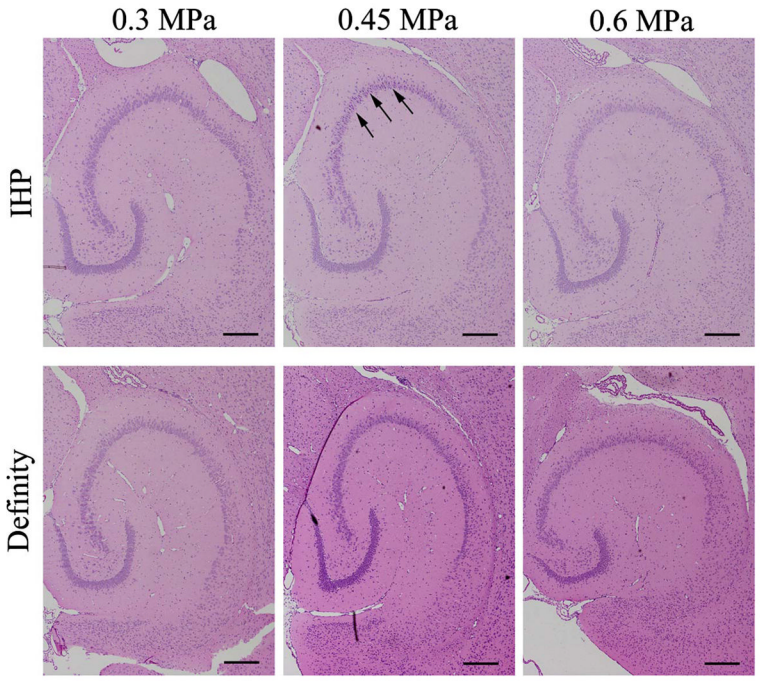


**Figure 6.**
Histological evaluation (H&E staining) of brains underwent FUS induced BBB opening (4X objective lens). No damage was observed except only one mouse from the in-house 22 polydisperse (IHP) group that was sonicated at 0.45 MPa (dark neurons are indicated by black arrows). All scale bars represent 500 μm.